# Roentgen stereophotogrammetric analysis to study dynamics and migration of stent grafts

Koning, O.H.J.

CHAPTER

8

# Assessment of 3-D stentgraft dynamics using fluoroscopic roentgen stereophotogrammetric analysis (FRSA)

Olivier H. J. Koning
Bart L. Kaptein
Eric H. Garling
Jan Willem Hinnen
Jaap F. Hamming
Edward R. Valstar
and J. H. van Bockel

*J Vasc Surg 2007;46:773-9*

## Abstract

**Objective:** To validate the use of Fluoroscopic Roentgen Stereophotogrammetric Analysis (FRSA) for its feasibility and accuracy to measure 3-D dynamic motion of stentgrafts.

**Methods:** A digital bi-plane fluoroscopy set-up was calibrated (Siemens Axiom Artis dBc®). Stereo images were acquired of a static aortic model with a stentgraft in different axial positions, imposed by a micromanipulator. The 3-D measurement error of FRSA was determined by comparing FRSA measurements to the micromanipulator. An aortic model with stent-graft was constructed and connected to an artificial circulation with a physiological flow and pressure profile. Markers were added to the spine (tantalum spherical markers, diameter 1mm) and stent (welding tin, diameter 1mm). 3-D measurement precision was determined by measuring the position of a single (stable) spine marker during 2 pulsatile cycles. Finally, 3-D stent marker motion was analyzed with a frame rate of 30 images per second, including 3-D marker position (change), diameter change, and center of circle position change.

**Results:** The mean error of FRSA measurement of displacement was 0.003mm (SD=0.019mm, max. error 0.058mm). A very high precision of position measurement was found (SD=0.009-0.015mm). During pulsatile motion, the position (changes) of the markers could be assessed in X, Y and Z direction, as well as stent diameter change and center of circle position change.

**Conclusion:** FRSA has proven to be a method with very high accuracy and temporal resolution to measure three dimensional stentgraft motion in a pulsatile environment. This technique has the potential to contribute significantly to the knowledge of stentgraft behavior after endovascular aneurysm repair and improvements in stentgraft design. The technique is ready for clinical testing.

## Introduction

Endovascular repair (EVAR) of an abdominal aortic aneurysm (AAA) is a widely used therapeutic alternative to open repair. A known problem with this technique is that the stentgraft can fail due to device defects caused by the continuous and significant forces of pulsatile blood flow. These failures have potential detrimental effects on patient health and safety.[1,2] An important problem of understanding failures is that it is difficult to study and measure aorta and stentgraft dynamics after EVAR, and clinical data are therefore limited. For the development, improvement and evaluation of new and current stentgrafts, it is of significant interest to understand aorta and stentgraft dynamics in vivo. Modeling of these blood flow related dynamics is very difficult. Subsequently, bench-testing of repetitive motion of stentgrafts is often inadequate and can lead to faulty stentgraft design.

Currently, cinegraphic CT and MRI can be used to measure aorta and stentgraft motion during the cardiac cycle.[3-5] An important limitation of these imaging modalities is that motion can only be measured in one plane. Three dimensional motion of specific points of a stentgraft cannot be quantified. Furthermore, the spatial resolution of these techniques is limited.[5]

Roentgen stereophotogrammetric analysis (RSA) is a tool to assess marker positions using stereo roentgen images.[6,7] This technique has proven to be highly accurate, and is used to measure prosthesis migration in the relative static environment of follow-up after joint replacement surgery.[8-11] Recently, RSA was introduced as an accurate tool to measure stentgraft migration during post-EVAR surveillance.[12,13] RSA can not be used to measure stentgraft motion during the cardiac cycle, since it uses one single stereo image acquired with two regular "single-shot" X-ray machines. It is therefore impossible to acquire a rapid sequence of calibrated images.

With the development of digital bi-plane fluoroscopic imaging systems, accurate measurement of three dimensional stentgraft motion during the cardiac cycle can become possible by combining stereo fluoroscopy with the RSA technique. This could enable in-vivo motion analysis of stentgrafts during the cardiac cycle. We validated the use of this combination of techniques: Fluoroscopic Roentgen Stereophotogrammetric Analysis, or FRSA, for its feasibility and accuracy to measure 3-D dynamic motion of stentgrafts.

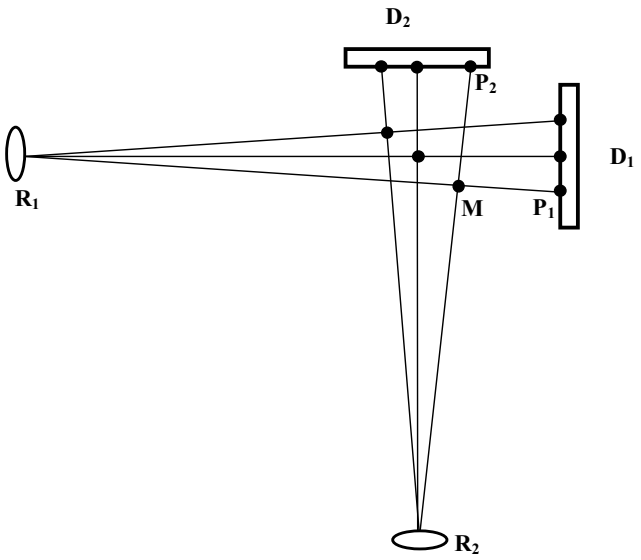


**Figure 1.** Schematic drawing of FRSA technique. The positions of the Roentgen foci ($R_1$ and $R_2$), the detectors (D1 and D2) and their relative position are known by calibration of the set-up. Graft markers give projections P and P' on the detectors. With a calibrated set-up, projection lines can be reconstructed. Calculation of intersections M of these projection lines in space gives the positions of the markers.

# Methods

## The concept of FRSA

Roentgen stereophotogrammetric analysis (RSA) is performed by calculating the point of intersection of two projection lines of a marker in space, using calibrated stereo Roentgen imaging (Figure 1). [6-13] FRSA uses high resolution digital stereo fluoroscopic images that are calibrated according to the same principles as RSA to calculate marker positions. Fast image acquisition and high frame rate theoretically enable accurate measurement of stentgraft motion in high spatial and temporal resolution.

## FRSA set-up

We used a Siemens Axiom Artis dBc imaging system (Siemens Nederland NV Medical Solutions, The Hague, The Netherlands) (Figure 2), which consists of two C-arms with digital flat panel Roentgen detectors. The focus to detector distance was set at 95 cm. The two C-arms were positioned at a 90 degree angle, to produce a posterior-anterior image and a lateral image. The images were acquired and stored in 1024 x 1024 pixels, 14 bits grey scale resolution (Figure 3). The frame rate was 30 bi-directional images per second. Each stereo image is acquired as two

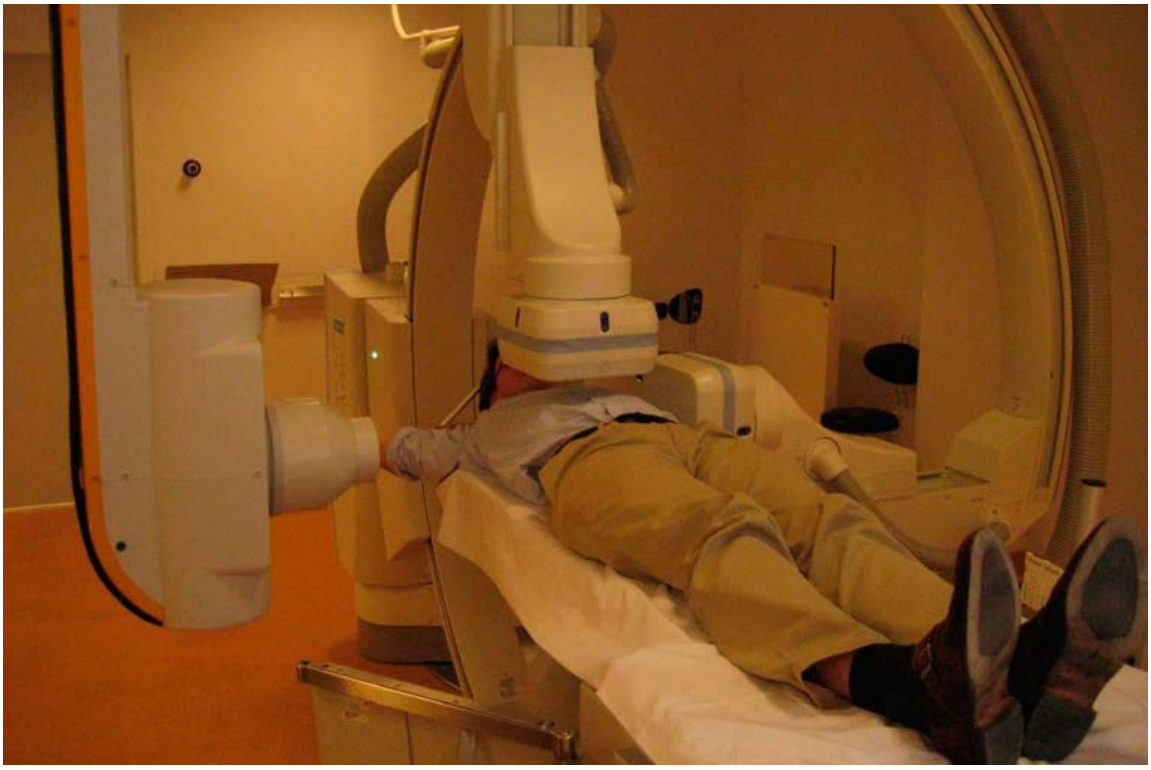

**Figure 2.** Clinical set-up of the bi-plane fluoroscope

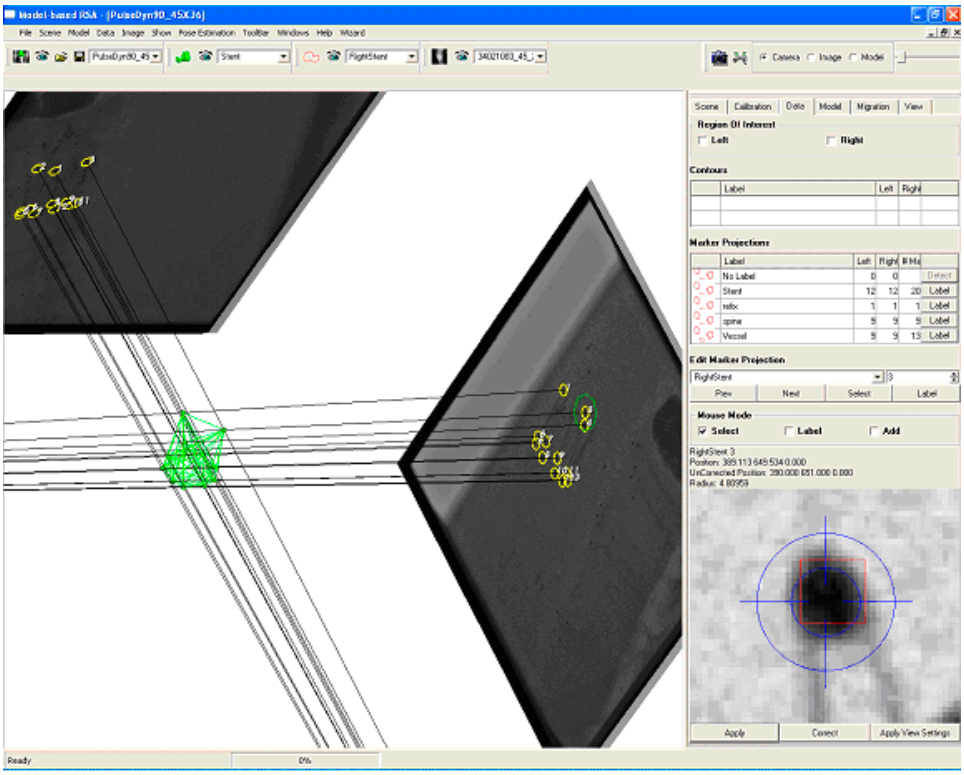


**Figure 3.** Image of the software with reconstruction of the stentgraft in space. The two images of a stereo image pair, a lateral and a postero-anterior image are visible. Right lower corner shows a detected stent marker.

separate alternating images, resulting in 60 alternating images per second. The exposure time of each image was 4 ms. The time between the posterior-anterior image and lateral image was 12.7 ms. For each analysis reported in this study, a 1.5 second run (45 stereo images) was acquired.

The image pairs were analyzed using Model-based RSA software (MB-RSA, MEDIS specials, Leiden, The Netherlands) to calculate the relative 3-D marker positions.[8-11] No image reconstruction is required before analyzing the image pairs.

## FRSA set-up calibration

To calibrate the set-up, a single focus run of a specially designed acrylic (PMMA, Vink Kunststoffen, Didam, The Netherlands) calibration box was acquired with each of the two C-arms.[14] From each run, a randomly chosen image was analyzed using the calibration algorithm as published previously.[14] This algorithm provides the calibration parameters to correct for image scale and geometric distortion, as well as the position of the Roentgen focus relative to the image for each C-arm. The relative position and orientation between the two C-arm images is necessary to calculate the 3-D marker positions using RSA analysis. This was achieved using a calibration object with 11 markers in known positions (Figure 4). The two images of the object were aligned to reconstruct the marker positions in space, reversing the calculation used to reconstruct an RSA image (Figure 1). This gave the position and orientation between the C-arms.

Further analysis of the experimental images as described below could now be performed within this calibrated set-up.

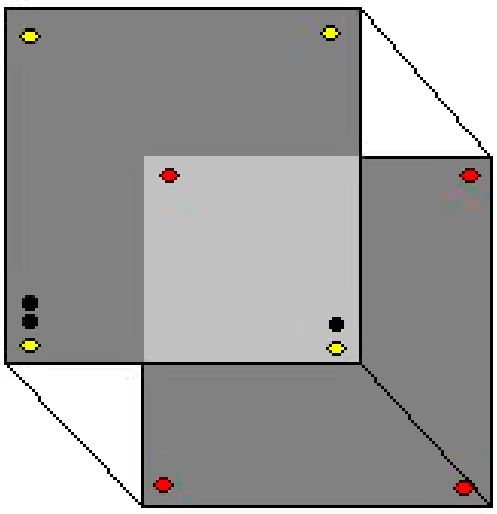

**Figure 4.** Calibration object. Plexiglas block, dimensions w x d x h: 8 x 8 x 5 cm. In every corner one tantalum marker, diameter 1mm (red and yellow). In the top layer three extra markers, diameter 2mm (black) for ease of identification of the different markers.

## Static model experiments

A static model of an aorta with stentgraft, with markers in known positions, was placed in the set-up (Figure 5). The same model was used as described previously.[12] The stentgraft could be translated accurately in the aorta lumen with a micromanipulator. The stentgraft was moved in axial direction inside the aorta over a distance of 1, 1.5 and 3mm, using the micromanipulator. The increments of the micromanipulator were accurate up to 0.01 mm according to the manufacturer, and confirmed by laboratory testing at our institution. The translation of the stent resulted in a 3D displacement of the markers. Three random stereo images were taken from an acquisition run of each position. Five marker positions were determined using FRSA. This was done to test for accuracy of measurement of the relative change in position of the markers by comparing the change in X, Y and Z coordinates and calculating the length of the resulting vector of displacement. Mean, standard deviation, minimum and maximum of the translations of the markers were measured and the results were compared to the micromanipulator settings, used as the standard of reference. This way, the measurement error of FRSA was determined for all measurements (n=45). These data were pooled to describe the mean error, standard deviation and maximum measurement error of marker position change as measured by FRSA.

**Figure 5.** Static model of an aorta (tube) with stentgraft (visible inside tube). Micromanipulator is on the left side.

## Pulsatile model experiments

For measurements under flow conditions, we developed a model to simulate a pulsating aorta with a stent-graft. To resemble human aorta characteristics, a fresh specimen of a porcine thoracic aorta was used, as published previously.[13] The porcine aorta was fixed to a human cadaver spine, replacing the cadaver aorta. The spine was complete with soft tissue (Figure 6). As an internal control for the experiments, the spine was marked with nine tantalum markers.

**Figure 6.** Pulsatile flow model. A fresh specimen of a porcine aorta was positioned ventral to a preserved human spine, complete with soft tissue. The porcine aorta replaced the human aorta. The aorta is connected to a pulsatile flow generator with physiologic flow and pressure profiles.

The aorta was filled with a starch solution with the same viscosity as blood. Inside the aorta, a Gianturco stent (Cook, Bjaeverskov, Denmark) was placed. The stent was marked with small drops of welding tin with a diameter of 1mm; the stent graft markers included nine at the cranial side and three at the caudal side. We used a stent rather than a stentgraft to study marker motion, since FRSA uses the stents of the stentgraft for analysis, identical to other radiological imaging techniques. The model was placed in a Plexiglas box, topped of with water to simulate soft tissue.

To test the feasibility to measure marker motion in a clinical situation, a study of a pulsating aorta was performed. The porcine – human aorta model was connected to an artificial circulation with a physiologic flow and pressure profile, as published previously.[13,15] This induced pulsatile marker motion of the aorta and stentgraft markers in X,Y and Z direction. With a pulse rate set at 80 per minute, a bi-plane fluoroscopy run of 1.5 sec resulted in imaging 2 pulsatile cycles. 3-D marker positions of the stent markers and the control markers in the spine were determined in every stereo image.

The tantalum spine markers were used to determine measurement precision. For each stereo image, the coordinates of a randomly chosen spine marker were determined (n=45). The X, Y and Z coordinates of the markers were compared to the average of the 45 measured positions and the standard deviation, minimum and maximum deviation were determined. This is a measure for the precision of the position estimation of a marker in consecutive stereo images using FRSA.

Finally, 3-dimensional stent marker motion was analyzed. The marker positions were determined for each sequential frame. The resulting series of marker positions was analyzed for

marker motion. Furthermore, a circle was estimated through the nine cranial markers in every stereo image. The resulting series of circles were analyzed for change of diameter (i.e. the stentgraft and inner vessel diameter) and motion of the circle center, as a measure for the three dimensional motion of the aorta – stentgraft complex. Analysis was performed with Matlab r2006B (The MathWorks, Natick, USA).

## Results

Using the calibration box, the set-up was tested for image distortion. No image distortion was found.

### Validation studies

The mean, standard deviation, minimum and maximum of the relative changes in position of the markers in the static stentgraft model are presented in Table 1. After pooling the measurement errors of FRSA, as compared to the micromanipulator, the mean error of 3D marker motion measurement by FRSA was 0.003mm, SD 0.019mm, maximum error 0.058mm (n=45). The precision of 3D marker position measurement by FRSA was determined by analysis of the position of one of the spine markers in 45 consecutive frames. The results are presented in Table 2. The precision is expressed by the standard deviation of the measured laboratory coordinates (0.009-0.015mm).

**Table 1.** 3D Changes in position (mm) of 5 markers measured by FRSA in 3 image frames (n=15 per displacement) compared to actual displacements as imposed by the micromanipulator which was applied as the "gold standard'.

| | | Imposed Translation | | |
|---|---|---|---|---|
| | | 1 mm | 1.5 mm | 3 mm |
| Measurements | Mean | 1.007 | 1.497 | 3.004 |
| | St Dev | 0.015 | 0.022 | 0.023 |
| | Min | 0.979 | 1.442 | 2.967 |
| | Max | 1.025 | 1.513 | 3.030 |

**Table 2.** Precision of position measurement of one spine marker in the 45 image frames (n=45).

| | X (mm) | Y (mm) | Z (mm) |
|---|---|---|---|
| St Dev | 0.015 | 0.009 | 0.012 |
| Min dev | -0.032 | -0.020 | -0.023 |
| Max dev | 0.027 | 0.017 | 0.027 |

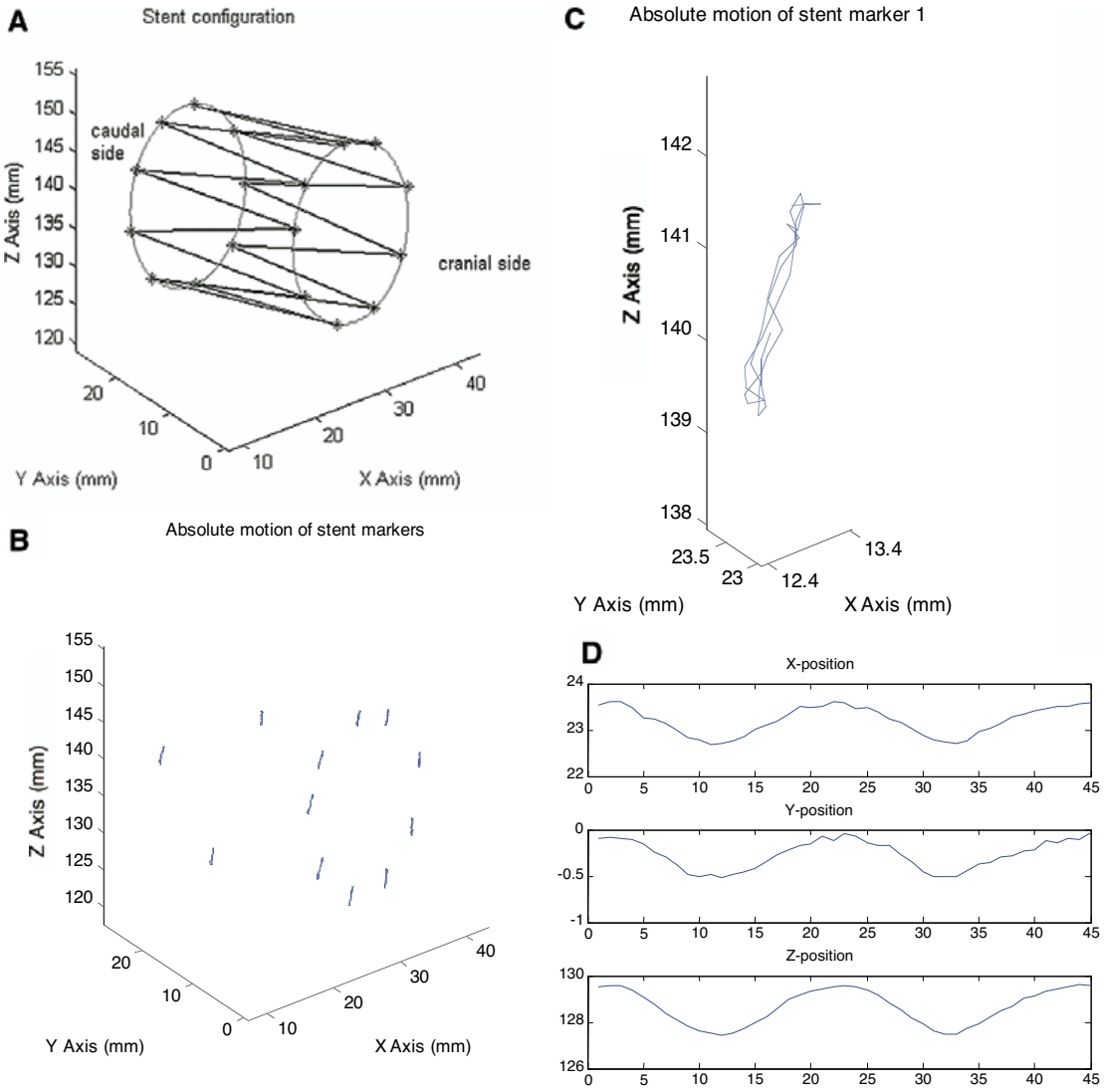


**Figure 7.** 3-D motion of the stentgraft markers. a) drawing of stent configuration. b) overview of the motion of twelve stentgraft markers, nine at the cranial side and three at the caudal side. c) 3D motion of a single stentgraft marker plotted in X, Y and Z direction. d) motion analysis of a stentgraft marker. break down in motion in X, Y and Z direction. X-axis depicts the images (1-45), Y-axis depicts the position relative to the laboratory coordinate system (in mm).

## Measurement of stentgraft dynamics

Finally, the pulsatile dynamics of the stentgraft were analyzed using the calibrated and validated set-up.

There appeared to be a cyclic motion of the stentgraft. This motion occurred in all directions. Figure 7a shows a schematic drawing of the stent configuration. Figure 7b shows the position (changes) of the stentgraft markers during the 2 pulsatile cycles (1.5 second acquisition run, 45 images). Figure 7c shows the position (changes) of a single marker during the same period. Figure 7d shows a break down of this marker motion in X, Y and Z direction.

Figure 8 shows the circle that was estimated through the cranial markers of the stentgraft. The cyclic diameter change of the circle is shown in Figure 9. The circle center motion is displayed in Figure 10, showing cyclic motion of the stent in all directions.

## Discussion

Fluoroscopic Roentgen Stereophotogrammetric Analysis (FRSA) enables highly accurate measurement of three dimensional motion of markers on a stentgraft in a pulsatile in-vitro model. Axial, lateral and rotational motion can be measured with a mean error of less than 0.01 millimeter, in every direction (error: 0.003mm, SD 0.019 ). The precision of 3D marker position measurement by FRSA is very high, expressed by the small standard deviation of the measurement of the X, Y and Z coordinates of the markers (0.009-0.015mm). This non-invasive technique enables quantifying clinical assessment of 3D-motion of a stentgraft in vivo at a high frame rate. This method is extremely important because the effects of pulsatile flow and stentgraft design on motion of the various stentgraft parts can be measured real time, in detail. Until now, this was impossible. FRSA may provide information that is crucial for further improvements in stentgraft design.

The use of CT and MRI for assessment of stentgraft motion has been reported, but these techniques are limited to the measurement of motion in a single plane.[3-5] Furthermore, the accuracy and reproducibility of these measurements have not been validated. This limitation to single plane analysis prevents analysis of complex motion patterns that occur differently in the various stentgrafts during the cardiac cycle, and include axial, transverse and rotational components.[3-5,16] This technical limitation of CT and MRI is caused by the fact that there currently is no technique available to follow a specific point (marker) of the graft in time through the 4D image data set. Moreover, application of MRI is limited by the fact that certain stentgrafts cause significant artifacts in MRI images.

Single focus fluoroscopic measurement of marker motion has been used to assess joint kinematics in orthopedic applications, using single plane images. This method is accurate parallel to the image plane (reported measurement error 0,1-0,17mm), but out of plane measurement error is relatively large (0,7-1,9mm).[14,17] Furthermore, this technique requires a fixed configuration of, at least 3, markers to enable reconstruction of the position of the implant. This fixed configuration cannot be achieved in the dynamic structure of current stentgrafts, making single focus fluoroscopy inappropriate for application in EVAR evaluation.

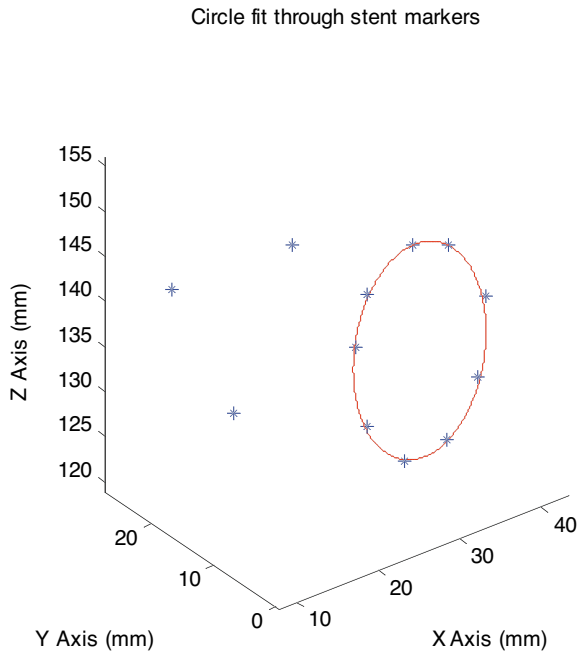


**Figure 8.** Circle fit through the nine cranial stent markers.

In this study, we used two sets of markers. One was the tantalum marker, a highly radiopaque, spherical marker, resulting in the best possible measurement in orthopedic RSA. This kind of marker could be added to the stentgraft by the manufacturer. The other marker we used was a drop of welding tin. These already occur in certain stentgrafts that are currently in wide clinical use. Markers that are used for positioning of the graft during EVAR can also be used for this procedure. Alternatively, automated pattern recognition of the stentgraft could be used to facilitate measurements without the need for markers. These aspects of FRSA are subject to further evaluation at our institution. In contrast to RSA, used to detect graft migration during follow-up [12,13], no additional markers are needed in the wall of the aorta to perform these dynamic measurements. The spine markers used in our study were solely used for this experiment to determine measurement precision and as an internal control. They were not used to determine the actual stent motion. The latter is done by independently reconstructing the position of each stent marker in space in the sequential images acquired by the calibrated set up, and calculating the marker displacement between these consecutive images.

## Limitations

A model was used to study pulsatile change in an aorta with a stentgraft. Patient studies have to be undertaken to assess the quality of the images and visibility of the markers of a stentgraft in vivo, surrounded by soft tissue. However, when considering the image quality of clinical

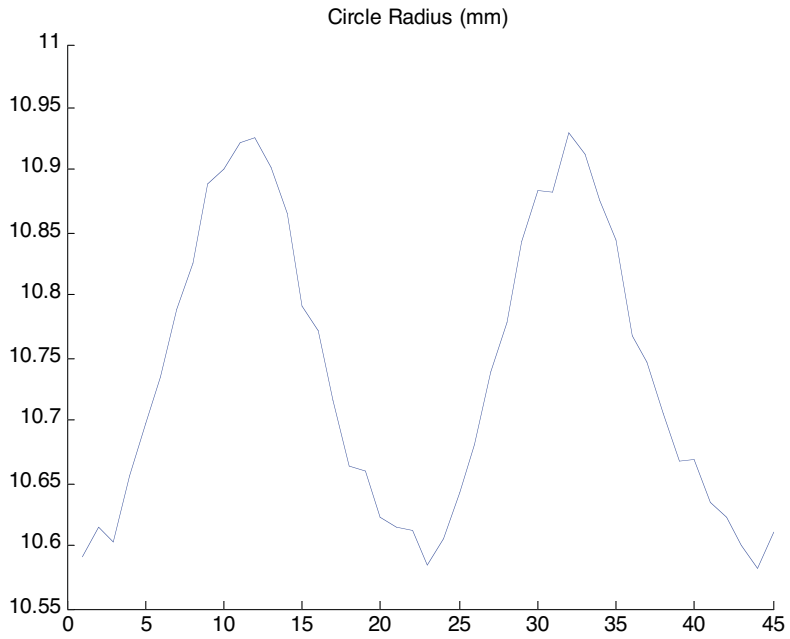


**Figure 9.** Change in radius of the circle in mm (Y-axis), as fitted through the 45 images (X-axis).

cardiovascular studies acquired by the Siemens set-up, and the validation of FRSA as demonstrated in this study, we are certain that analysis of patient images is feasible, and therefore analysis of stentgraft motion in-vivo can be performed.

Different commercially available stentgrafts bare different markers. In this study only one graft design was tested. Based of our experience with RSA, including pilot testing of imaging and detectability of markers on different commercially available stentgrafts, we believe that motion analysis of different commercially available grafts is feasible. This issue is subject to further study at our institution.

## Practical applications

Further, detailed, knowledge of stentgraft motion during the cardiac cycle is required to better understand in-vivo behavior of stentgrafts after EVAR. New stentgrafts can be evaluated, as well as existing grafts. With this knowledge, virtual mechanical modeling becomes possible and assessment of the failure modus of the stentgraft, such as failure due to metal fatigue is facilitated. Based on clinically acquired, detailed knowledge of stentgraft motion, forces acting on the stentgraft during the cardiac cycle can be calculated more accurately. With this knowledge, it is possible to evaluate pre-clinical bench testing of stentgrafts and verify its adequacy. Bench testing itself will be improved according to in-vivo measured clinical data. Knowledge of in-vivo stentgraft motion should be an important adjunct in phase I clinical evaluation of

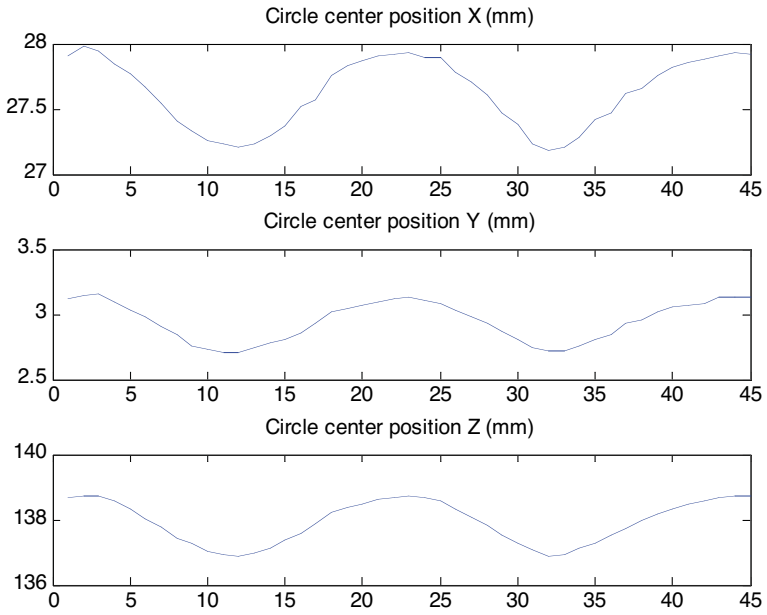


**Figure 10.** Change of position of the circle center. X-axis depicts the images (1-45), Y-axis depicts the position relative to the laboratory coordinate system (in mm).

stentgrafts. Withdrawal of a graft from the market due to mechanical defects that arise after widespread introduction could be prevented with better bench testing and early detection of unexpected graft motion.

The radiation dose of FRSA was determined in a separate, unpublished experiment by our clinical physicists. The radiation dose is approximately 0.1 mSv for a 3 second study, which corresponds to 4 cardiac cycles at a heart rate of 80 bpm. This compares very favorable to the 17 mSv dose of triple phase CT scan used for EVAR follow up.

## Conclusion

In this study, FRSA has proven to be a method with very high accuracy and temporal resolution to measure three dimensional stentgraft motion in a pulsatile environment. This technique has the potential to contribute significantly to the knowledge of stentgraft behavior after endovascular aneurysm repair and improvements in stentgraft design. The technique is ready for clinical testing.

## Acknowledgements

We would like to acknowledge the help of the following persons:

M.J. Schalij, MD, Interventional Cardiologist, Department of Cardiology, LUMC, for his assistance with the image acquisition.

M. Boonekamp, Department of Fine Mechanics, LUMC, for his assistance in building the models and the calibration object.

J. Geleijns, MSc, PhD and P.W. de Bruin, MSc, PhD, Clinical Physics, Department of Radiology, for their work on radiation dose measurement of FRSA.

# References


1. Bockler D, von Tengg-Kobligk H, Schumacher H, Ockert S, Schwarzbach M, Allenberg JR. Late surgical conversion after thoracic endograft failure due to fracture of the longitudinal support wire. J Endovasc Ther. 2005 Feb;12(1):98-102.

2. Jacobs TS, Won J, Gravereaux EC, Faries PL, Morrissey N, Teodorescu VJ, et al. Mechanical failure of prosthetic human implants: a 10-year experience with aortic stent graft devices. J Vasc Surg. 2003 Jan;37(1):16-26.

3. Verhagen, HJ, Teutelink A, Olree M, Rutten A, de Vos AM, Raaijmakers R, et al. Dynamic CTA for cutting edge AAA imaging: Insights into aortic distensibility and movement with possible consequences for endograft sizing and stentdesign *J Endovasc Ther*. 2005;12:I-45.

4. Teutelink A, Rutten A, Muhs BE, Olree M, van Herwaarden JA, de Vos AM, et al. Pilot study of dynamic cine CT angiography for the evaluation of abdominal aortic aneurysms: implications for endograft treatment. J Endovasc Ther. 2006 Apr;13(2):139-44.

5. Vos AW, Wisselink W, Marcus JT, Vahl AC, Manoliu RA, Rauwerda JA. Cine MRI assessment of aortic aneurysm dynamics before and after endovascular repair.*J Endovasc Ther* 2003;10:433-9.

6. Selvik G. Roentgen stereophotogrammetry. A method for the study of the kinematics of the skeletal system. *Acta Orthop Scand Suppl*. 1989;232:1-51.

7. Karrholm J. Roentgen stereophotogrammetry. Review of orthopedic applications. *Acta Orthop Scand*. 1989;60:491-503.

8. Valstar ER, Vrooman HA, Toksvig-Larsen S, Ryd L, Nelissen RG. Digital automated RSA compared to manually operated RSA. *J Biomech*. 2000;33:1593-1599.

9. Vrooman HA, Valstar ER, Brand GJ, Admiraal DR, Rozing PM, Reiber JH. Fast and accurate automated measurements in digitized stereophotogrammetric radiographs. *J Biomech*. 1998;31:491-498.

10. Valstar ER, de Jong FW, Vrooman HA, Rozing PM, Reiber JH. Model-based Roentgen stereophotogrammetry of orthopaedic implants. *J Biomech*. 2001;34:715-722.

11. Kaptein BL, Valstar ER, Stoel BC, Rozing PM, Reiber JAC. A new model-based RSA method validated using CAD models and models from reversed engineering. *J Biomech*. 2003;36:873-882.

12. Koning OH, Oudegeest OR, Valstar ER, Garling EH, van der Linden E, Hinnen JW, et al. Roentgen Stereophotogrammetric Analysis: an accurate tool to assess endovascular stentgraft migration. *J Endovasc Ther.* 2006;13:468-475

13. Koning OH, Garling EH, Hinnen JW, Kroft LJ, van der Linden E, Hamming JF, et al. Accurate detection of stentgraft migration in a pulsatile aorta using Roentgen Stereophotogrammetric Analysis. *J Endovasc Ther.* 2007;14(1):30-8.

14. Garling EH, Kaptein BL, Geleijns K, Nelissen RG, Valstar ER. Marker Configuration Model-Based Roentgen Fluoroscopic Analysis. J Biomech. 2005;38(4):893-901.

15. Hinnen, JW, Visser MJ, Van Bockel JH. Aneurysm sac pressure monitoring: effect of technique on interpretation of measurements. *Eur J Vasc Endovasc Surg* 2005; 29:233-8

16. Flora HS, Woodhouse N, Robson S, Adiseshiah M. Micromovements at the aortic aneurysm neck measured during open surgery with close-range photogrammetry: implications for aortic endografts. *J Endovasc Ther*. 2001;8:511-520.

17. Ioppolo J, Borlin N, Bragdon C, Li M, Price R, Wood D, et al. Validation of a low-dose hybrid RSA and fluoroscopy technique: Determination of accuracy, bias and precision. *J Biomech*. 2007;40(3):686-92.